Electrostatic Interaction of a K^+ Channel RCK Domain with Charged Membrane Surfaces†

Christopher P. Ptak, Luis G. Cuello, and Eduardo Perozo*

Department of Molecular Physiology and Biological Physics, Center for Structural Biology and Biophysics Program, University of Virginia Health Sciences Center, Charlottesville, Virginia 22908

Received July 28, 2004; Revised Manuscript Received October 27, 2004

ABSTRACT: In a subset of K^+ channels, gating is regulated through the direct binding of ligands by large cytoplasmic RCK domains. To further investigate the role of the RCK domain, we have begun the biochemical characterization of a two-transmembrane segment, RCK domain-containing channel from *Methanococcus jannaschii*, MjK2, by testing its general functional behavior and identifying purification conditions. Standard detergent solubilization of recombinantly expressed MjK2 required the addition of a high NaCl concentration to the extraction buffer for MjK2 solubilization. The cytoplasmic RCK domain was identified as the region of MjK2 responsible for the dependence of solubilization on high salt concentrations since expression of an MjK2 construct lacking the transmembrane domain, MjK2cd, also required high salt concentrations for extraction from *Escherichia coli* lipids, a necessary step in the purification of both MjK2 and MjK2cd. MjK2 expression was able to weakly recover growth of K^+ uptake deficient LB2003 cells at 10 mM KCl, suggesting that the channel can conduct K^+ but has a low open probability. Purified MjK2 reconstituted in liposomes generated only limited Rb^+ uptake, blocked by $BaCl_2$. MjK2cd exhibited direct binding to PC/PS lipid vesicles with a molar partition coefficient (K_1) of $\approx 10^3$ M^{-1}, which decreased with both an increase in the salt concentration and a decrease in the anionic lipid ratio. Lipid blot assays revealed that MjK2cd binds most strongly to lipids of increasingly negative charge. These results support the idea that the binding of the MjK2 RCK domain to membranes takes place via an electrostatic interaction with anionic lipid surfaces.

Potassium channels are present in most cell types from a wide range of organisms (*1*). The great diversity of K^+ channels allows them to serve a variety of cellular functions. Effectors ranging from transmembrane voltage to membrane tension can selectively activate ion channels. Increasingly, membrane-bound effectors are being shown to be important in channel regulation. Inward rectifier K^+ (Kir) channels rely heavily on membrane-delimited pathways for control of opening. Membrane-bound G-proteins and the signaling lipid, PIP_2, both increase activity of certain Kir channels (*2*−*5*). The cytoplasmic portion of some Kir channels has been shown to bind PIP_2 in the absence of the channel transmembrane domain (*6*). In addition, the mutation of residues involved in PIP_2 binding has been implicated in the development of genetic diseases such as Andersen's and Bartter's syndromes (*7*).

At a molecular level, ion conduction through tetrameric K^+ channels revolves around a common core domain, but channel regulation is controlled by an assortment of domains with a variety of structures. For bacteria, common regulatory domains are the RCK (regulates conductance of K^+) and the closely related KTN (K^+ transport, nucleotide binding) domain, which have both been found within the primary sequence or as an accessory subunit of a number of K^+ channels and transporters (*8*, *9*). Bacterial genomes often include many genes containing RCK/KTN domains, emphasizing the importance of this domain family in prokaryotic physiology.

The structure of the *Escherichia coli* K^+ channel's RCK domain (*10*) and then the subsequent structure of a complete RCK domain-containing channel, MthK (*9*), reveal a dimeric nature which may form a complicated octameric ring. Such an octamer is derived from alternating RCK domains that are linked to channels and cytoplasmic RCK domains that are expressed at a second start methionine just after the channel's last transmembrane helix (Figure 1A,B) (*9*). The RCK and KTN domains adopt the same basic fold except for a conserved sequence of residues, GXGXXG, found only in the KTN domain's ligand-binding pocket, suggestive of its ability to bind nucleotides (*11*). Crystal complexes of KTN domains have been observed with bound dinucleotides, but the MthK RCK domain contains Ca^{2+} bound to the activated complex (*9*, *11*). The pocket is thought to be versatile in structure, allowing it to incorporate specificity for many different ligands.

The structural and regulatory complexity of the RCK/KTN domain and its importance in the ion channel field are just now being realized. Interestingly, RCK-like domains are also found in eukaryotic channels as a core structural component of the BK_{Ca} family (*10*) and have been implicated in

† This research was supported by grants from the National Institutes of Health and the McKnight endowment fund for neuroscience.

* To whom correspondence should be addressed. Telephone: (434) 243-6580. Fax: (434) 982-1616. E-mail: eperozo@virginia.edu.

10.1021/bi048390f CCC: $30.25
Published on Web 12/13/2004

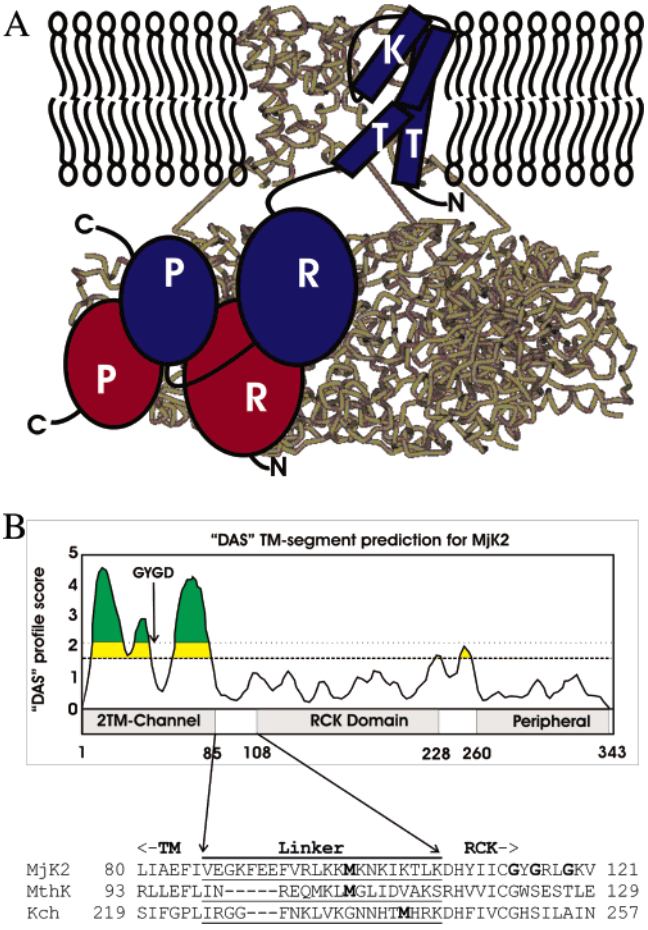

FIGURE 1: (A) Multimeric structure of MthK depicted as a Cα tube with the transmembrane domain positioned in a bilayer. From the tetramer, one heterodimeric subunit was removed and replaced with a cartoon. The domains within MthK are labeled with letters (T, transmembrane segments; K, K^+ selective pore; R, RCK domain; P, peripheral subdomain). MthK is composed of two products expressed by the same gene: the entire gene product containing all domains (blue) and the cytoplasmic RCK domain, which is expressed from an internal start site (red). The N- and C-termini of each gene product are defined. (B) A "DAS" transmembrane prediction for MjK2 shows the location of the two predicted helices in green, which surround the GYGD signature sequence for K^+ channels. The relative location of protein domains along the primary sequence of MjK2 is correlated with the DAS plot. An alignment of the linker region between the transmembrane domain and the RCK domain contains the second methionine start sites for MjK2−2TM (GenBank entry 2493596), MthK−2TM (GenBank entry 21542150), and *E. coli* Kch−6TM (GenBank entry 400124). Also, the GXGXXG signature sequence for nucleotide binding is located at the beginning of the RCK domain.

tetramerization and Ca^{2+} activation (*12*−*14*). Recently, three putative archaeal K^+ channels from *Methanococcus jannaschii*, MVP (Mj0139), MjK1 (Mj0138.1), and MjK2 (Mj1357), were identified and functionally characterized (*15*, *16*). In this paper, we focus our efforts on the biochemical characterization of MjK2, a two-transmembrane helix channel with a C-terminal RCK domain, for future structural analyses. MjK2 contains the conserved sequence for KTN domains (Figure 1B); however, we will refer to the cytoplasmic domain as an RCK domain in this paper due to MjK2's high degree of similarity to MthK. Here, we show an electrostatic interaction between the RCK domain and anionic lipids. Similar interactions existing in eukaryotic Kir channel cytoplasmic domains suggest that channel regulatory domain−anionic lipid interactions may also be a common theme in the physiology of prokaryotic channels.

MATERIALS AND METHODS

Molecular Biology and Expression. The orf Mj1357 was amplified from *M. jannaschii* genomic DNA (American Type Culture Collection, Manassas, VA) and cloned into pQE32 (between enzyme cut sites BamHI and HindIII) and pQE70 (between enzyme cut sites SphI and BamHI) expression vectors (Qiagen, Valencia, CA). The MjK2cd construct (residues 106−343) encoded the cytoplasmic RCK domain and was cloned by PCR from the MjK2 channel clone into pQE32 between SphI and SalI. QuickChange mutagenesis (Stratagene, La Jolla, CA) was used to create MjK2 site-directed mutants. For expression tests, MjK2 and MjK2 (M99L) cloned into pQE70 were transformed into SG-13 cells. Cells were grown and induced with 0.5 mM IPTG and grown for an additional 2 h before collection. The cell pellets lysed with 3% SDS[1] were run on a 15% SDS−PAGE gel. ECL reagents (Amersham Biosciences) were used to visualize the gel immunoblotted with Penta-His Antibody (Qiagen).

K^+ Uptake Complementation. Competent LB2003 cells with pREP4 (Qiagen) were transformed with the pQE70 or pQE32 vector containing MVP, MjK2, MjK2 (M99L), MjK2cd, or nothing. A 1 mL aliquot of overnight culture (OD_{600} = 3) grown in LB medium (Invitrogen, Carlsbad, CA) supplemented with 100 mM KCl, kanamycin, and ampicillin was centrifuged and washed twice in KML medium lacking K^+. The KML medium was formulated as previously described (*17*) with the combined K^+ and Na^+ concentration totaling 115 mM. Serial dilutions made in KML media at 10^2, 10^3, 10^4, 10^5, and 10^6 were then plated in 5 μL aliquots onto KML agar media at fixed K^+ concentrations. Plates were incubated at 37 °C until colonies formed (~3 days).

Salt Extraction Experiments. MjK2 cloned into pQE70 or pQE32 was expressed as described above, while MjK2cd in pQE32 was transformed into XL1-Blue cells before expression. Cells were homogenized using a French pressure cell, and the membrane-containing fraction was collected; 5 μL of the insoluble fraction was incubated with 200 μL of extraction buffer with varying NaCl concentrations [5 mM Na_2PO_4 (pH 7)]. The extraction buffer for MjK2 also contained 6 mM dodecyl maltoside (DDM) (Anatrace, Maumee, OH). After centrifugation, the upper 100 μL of buffer was collected and run on a 15% SDS−PAGE gel. Protein bands on the gels were detected using Coomassie stain. Scanned gels were analyzed using Scion Image (Scion Corp., Frederick, MD), and data were fit to sigmoidal curves. Purification of MjK2 in pQE70 from cell membrane paste

[1] Abbreviations: DDM, dodecyl D-maltoside; OG, octyl D-glucoside; Mega 9, nonanoyl *N*-methylglucamide; C8E4, *n*-octyltetraoxyethylene; DOC, deoxycholate; SDS, lauryl sulfate; CHAPS, 3-[(3-cholamidopropyl)dimethylammonium]-1-propanesulfonate; IPTG, isopropyl thiogalactoside; CMC, critical micellar concentration; PG, phosphatidylglycerol; LPC, lysophosphatidylcholine; PC, phosphatidylcholine; PE, phosphatidylethanolamine; PS, phosphatidylserine; S1P, sphingosine phosphate; $PI(3,4)P_2$, phosphatidylinositol 3,4-bisphosphate; $PI(3,5)P_2$, phosphatidylinositol 3,5-bisphosphate; $PI(4,5)P_2$, phosphatidylinositol 4,5-bisphosphate; PIP_3, phosphatidylinositol triphosphate; PA, phosphatidic acid; LPA, lysophosphatidic acid; PI, phosphatidylinositol; PI(3)P, phosphatidylinositol 3-phosphate; PI(4)P, phosphatidylinositol 4-phosphate; PI(5)P, phosphatidylinositol 5-phosphate.

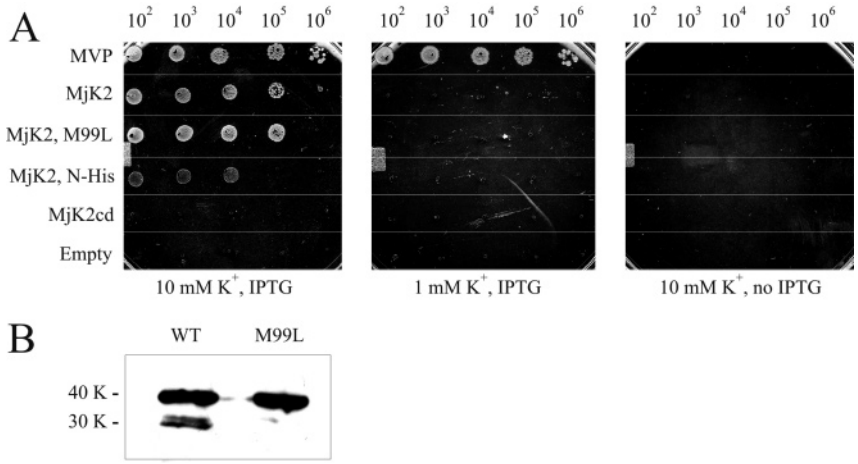

FIGURE 2: Functional complementation of LB2003 cells by different ion channel constructs. (A) Experiments with pQE70 vectors containing MVP (lane 1, positive control), MjK2cd (lane 5, negative control), nothing (lane 6, negative control), MjK2 (lane 2), and MjK2 M99L (lane 3) and MjK2 in pQE32 (lane 4) were conducted on KML plates with 10 mM KCl with or without IPTG or with 1 mM KCl and IPTG. Serial dilutions in 5 μL aliquots were spotted onto the plates. Plates were incubated for 3 days before being scanned. (B) Cell pellets containing expressed MjK2 and MjK2 M99L with a C-terminal six-His tag were separated by SDS−PAGE and immunoblotted with the anti-His antibody.

was achieved with an initial wash with high-salt buffer [500 mM NaCl, 100 mM KCl, and 5 mM Na_2PO_4 (pH 7)] and centrifuged to remove the excess RCK domain. The washed pellet was incubated in high-salt buffer containing 6 mM DDM and centrifuged again to yield a solubilized fraction containing MjK2. The Co^{2+} metal−chelate resin (Clontech, Palo Alto, CA) was used to bind the C-terminal His-tagged MjK2, which was eluted with 0.5 M imidazole in high-salt buffer containing 1 mM DDM. The purified protein was run on a Superdex-200 gel filtration column (Amersham Biosciences) in high-salt phosphate buffer containing 1 mM DDM.

Rb^+ Flux Assay. Purified MjK2 or KcsA was reconstituted into asolectin liposomes. $^{86}Rb^+$ fluxes were performed using the protocol previously described for KcsA (*18*). Vesicles containing $^{86}Rb^+$ were assessed using a scintillation counter.

Liposome Binding Assay. Binding experiments involved mixing a small amount of protein with increasing concentrations of vesicles and centrifuging off the vesicles and any protein that binds (*19*). Charged and neutral lipids obtained from Avanti Polar Lipids (Alabaster, AL) were mixed and dried at the desired ratios. To ensure that vesicles could be easily centrifuged out of solution, they were formed with an internal solution containing sucrose and extruded to a constant size of 0.1 μm. The external solution was replaced with a salt solution of the same osmolarity. MjK2cd was extracted from lysed cell pellets using high-salt buffer and centrifuged. The supernatant was poured over the Co^{2+} metal−chelate resin, and MjK2cd was isolated by elution with 0.5 M imidazole in high-salt buffer. Circular dichroism (CD) spectra of MjK2cd were obtained on an Aviv (Lakewood, NJ) 215-CD spectrometer. Purified MjK2cd was labeled with the cysteine reactive fluorophore, 7-(diethylamino)-3-(4′-maleimidylphenyl)-4-methylcoumarin (CPM) (Molecular Probes, Eugene, OR). CPM-labeled MjK2cd was mixed with sucrose-loaded vesicles over a range of concentrations and centrifuged. The fluorescence intensity of the unbound protein, which was measured with a Shimadzu spectrofluorophotometer (RF-1501), was used to determine the fraction of protein bound to the membrane. Curves were fit to the plots of the lipid vesicle concentration, [L], against the fraction of protein bound to the membrane, f_b, using the equation $f_b = K[L]/(1 + K[L])$. The partition coefficient was determined as the reciprocal of the apparent dissociation constant, K_d. The effects of salt concentration on binding were analyzed at a PC:PS ratio of 2:1 and a vesicle concentration of 8 mM. Experiments on anionic lipid ratio were carried out at 150 mM NaCl and at a vesicle concentration of 8 mM. Sigmoidal curves were fit to plots versus salt or anionic lipid concentration.

Lipid Specificity Screen. Strips of nitrocellulose spotted with various lipids were either obtained from Echelon (Salt Lake City, UT) or generated by spotting 5 μL of lipid in chloroform onto a nitrocellulose strip. A protein overlay was performed as described previously (*20*). The lipid strips were incubated with MjK2cd, then with Penta-His antibody (Qiagen), and finally with horseradish peroxidase-conjugated anti-mouse antibody. ECL reagents (Amersham Biosciences) were used to detect spot intensities.

RESULTS

K^+ Channel Activity of MJK2. *E. coli* cell strain LB2003 lacking the K^+ uptake systems, Kdp, Kup, and Trk, has become a useful tool in assessing the ability of cloned channels to function in an *E. coli* cell membrane. LB2003 cells fail to grow at low potassium levels but are able to grow normally when the growth medium is supplemented with 100 mM KCl. The ability to grow at low potassium levels can be recovered by the heterologous expression of potassium channels that allow for the leak of potassium into the cells. The voltage-gated potassium channel, MVP, is open when expressed in *E. coli* and can recover growth on media containing as little as 1 mM KCl and was able to serve as a positive control in our experiments (Figure 2A) (*16*, *21*). The pREP4 vector was introduced into the LB2003 strain to fully suppress expression of any channel in the absence of IPTG, and no growth was observed without the addition of IPTG (*22*). The pQE70 vector alone and the soluble RCK domain (MjK2cd) served as the negative control.

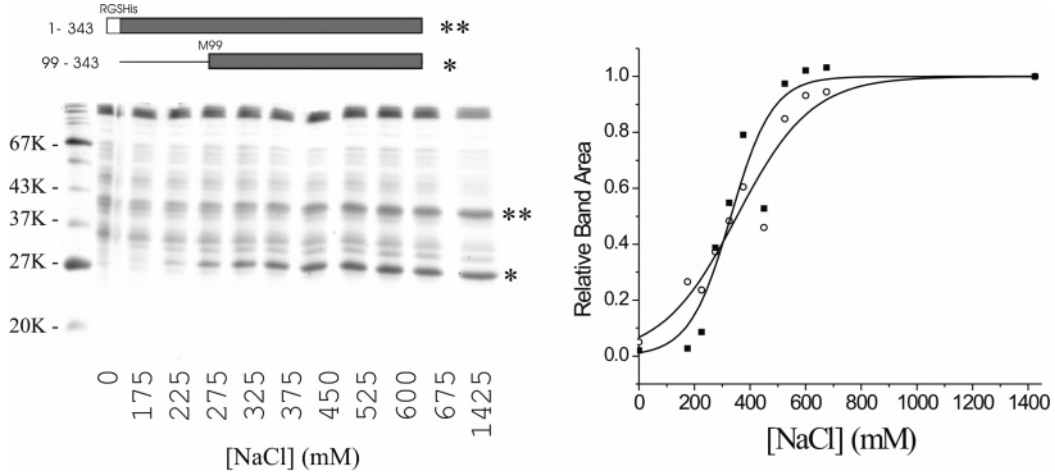

FIGURE 3: Effect of an increase in the NaCl concentration on MjK2 in 6 mM dodecyl maltoside during solubilization. MjK2 in pQE32 was extracted from the pelleted cell lysate by increasing the NaCl concentration of the solubilization buffer and visualized on a Coomassie-stained gel. Both the MjK2 (two asterisks) (40 kDa) and the second gene product (one asterisk) (30 kDa) are extracted by an increase in the NaCl concentration. The product of the intensity and the area of the bands at each NaCl concentration is related to the protein concentration and was plotted to determine the relative efficiency of solubilization. A sigmoidal curve was used to fit both the MjK2 (○) (40 kDa) and the second gene product (■) (30 kDa).

Expression of MjK2 in LB2003 cells did not allow growth on media containing 1 mM KCl; however, it was able to recover growth at 10 mM (Figure 2A, lane 2). Although the ability of MjK2 to weakly rescue potassium uptake in LB2003 cells suggests that MjK2 is creating a pathway for some potassium to enter the cells, it does so at a fairly high K^+ concentration, suggesting that the channel is functionally closed or has a very low open probability. We note that MjK2 expressed with an N-terminal His tag instead of a C-terminal tag is less able to recover LB2003 cells (Figure 2A, lane 4).

Similar to the MthK and Kch potassium channels, the MjK2 gene is able to produce protein products from both the primary methionine start site (40 kDa, M1) and an internal start site just before the RCK domain (30 kDa, M99) (Figures 1B and 2B) (*9*, *23*). Using Western blot analysis, the 40 and 30 kDa gene products can be visualized with anti-His antibodies since both proteins contain the C-terminal histidine tag. A mutation of methionine 99 to leucine (M99L) removes the 30 kDa protein on the Western blot analysis. The M99L mutant was also tested for the ability to rescue the LB2003 cells, and no difference was found between the MjK2 gene with or without the 30 kDa protein, suggesting that the second gene product is not necessary for maintaining a closed tetrameric channel (Figure 2A, lane 3).

Solubilization of MjK2. MjK2 was expressed in *E. coli*, and attempts were made to solubilize MjK2 with a detergent screen consisting of the following detergents at 10 times their respective CMCs: APO 8-12, C8E4, CHAPS, dodecyl maltoside (DDM), DOC, FOS-choline 8-16, LDAO, Lubrol, Mega-9, octyl glucoside, Pluronic F-127 and P-85, SDS, Triton, and Tween 20. All detergents, with the exception of SDS, were unable to extract a significant percentage of MjK2 from a lysed cell membrane preparation using standard ionic conditions (PBS buffer at pH 7). High salt was tested as an additive and was found to greatly enhance the ability of most detergents to extract the channel. Coomassie gels show the solubilization of an MjK2 lysed cell pellet after incubation with 6 mM DDM and increasing amounts of NaCl (Figure 3). It was also observed that a second protein band, corresponding to the second RCK gene product (30 kDa), also increases in intensity at higher salt concentrations. The salt extraction plots are similar for either an N- or C-terminally tagged channel; however, Figure 3 shows an N-terminally tagged channel to illustrate that the second open reading frame lacking a His tag still requires high salt concentrations for extraction. Both (40 and 30 kDa) protein bands were positively identified on a complementary Western blot and also using tandem mass spectrometry on an LCQ deca mass spectrometer (*24*) (Thermoelectron, San Jose, CA). Thus, to facilitate the purification of MjK2, the free RCK domain was first removed with a high-salt wash followed by an extraction of MjK2 with DDM and high salt. Further purification of MjK2 was achieved by metal affinity chromatography, yielding a gel filtration peak at 10.9 mL, which is similar to the gel filtration behavior of MthK (*9*) (Figure 4A). The final yield of the MjK2 purification was ~1−2 mg/L of cells.

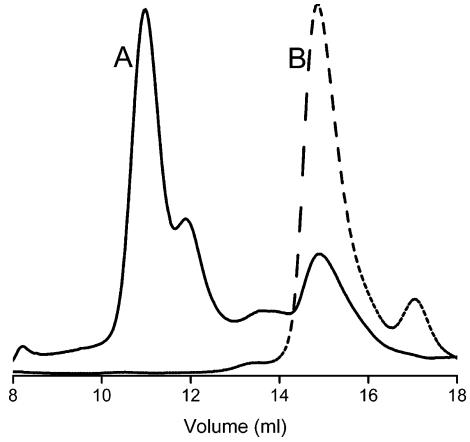

FIGURE 4: Gel filtration of purified MjK2 and MjK2cd. The metal affinity-purified protein was run on a Superdex-200 in a high-salt buffer. MjK2 eluted at 10.9 mL (A), while MjK2cd eluted at 14.8 mL (B).

Functional Analyisis of MjK2. Attempts were made to characterize the function of purified MjK2 using a Rb^+ concentrative flux assay (*18*, *25*). Liposomes containing reconstituted MjK2 were capable of very limited Rb^+ uptake, although this uptake was blocked by the addition of 10 mM

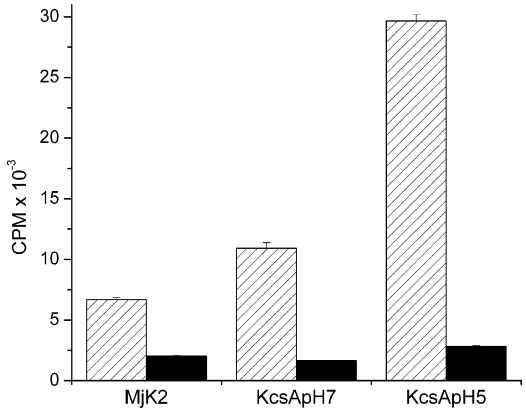

FIGURE 5: Rb^+ fluxes for MjK2. The purified channel was reconstituted into asolectin liposomes, and the uptake of $^{86}Rb^+$ was assessed. Rb^+ fluxes (hatched bars) and 10 mM $BaCl_2$ blocked fluxes (black bars) are plotted for MjK2, KcsA at pH 7 (closed), and KcsA at pH 5 (open).

$BaCl_2$, adding further support to the notion that MjK2 can function as a K^+ channel (Figure 5). MjK2 Rb^+ fluxes were comparable to those of KcsA at neutral pH, where the channel is marginally open, and much smaller than those expected from KcsA at pH 5.0. Thus, under the conditions of these experiments, MjK2 likely populates a mostly closed conformation.

Solubilization of MjK2cd. To help determine the role of the cytoplasmic domain of MjK2 in its solubilization behavior, we made a construct, MjK2cd, which lacks the predicted transmembrane domains (*26*) (Figure 1). The expression of MjK2cd produced a protein that fails to solubilize from the *E. coli* membrane at an ionic strength of 150 mM. Again, increasing the amount of NaCl improved the MjK2cd extraction from the lysed cell pellet, and only NaCl concentrations above 300 mM were able to keep the expressed protein in solution (Figure 6). The failure of buffers with increased solute levels (glucose or glycine) to keep MjK2cd in solution excluded the possibility of an osmotic effect by NaCl. In addition, the possible effect of inclusion bodies on the extraction was discounted since a similar NaCl extraction curve for MjK2cd could be obtained after removal of low-speed debris (10000*g*) from the lysed cell pellet. MjK2cd was extracted from the *E. coli* membrane lysate with 0.5 M NaCl. The elution volume for the peak of MjK2cd from gel filtration was 14.8 mL (Figure 4B) with a final protein yield of ~10−15 mg/L of cells. Circular dichroism (CD) spectroscopy was used to characterize the secondary structure in solution. The CD spectra did not change for NaCl concentrations between 0.1 and 0.5 M (Figure 7); however, upon addition of 2−6 M urea, we found the expected decrease in negative absorbance at 222 nm, suggesting protein unfolding and the loss of secondary structure. The secondary structure of MjK2cd using NPS@ (*27*) was estimated to be 40−49% α-helix and 13−23% β-sheet and is comparable to the secondary structure calculated using SELCON3 for the MjK2cd CD spectra (56% α-helix and 11% β-sheet) (*28*, *29*). Our CD spectra for MjK2cd support proper folding under the conditions used in this study.

Liposome Binding. Purified MjK2cd was fluorescently labeled and tested for its ability to bind to liposomes containing anionic lipids. The percentage of unbound MjK2cd was measured under varying lipid concentrations, percents of anionic lipid, and NaCl concentrations. At increasing lipid concentrations, a larger fraction of MjK2cd is bound to the liposomes (Figure 8A). MjK2cd binds to 2:1 PC/PS vesicles in 150 mM NaCl with a molar partition coefficient (K_1) of 1.9×10^3 M^{-1} ($K_1 = 1.8 \times 10^2$ M^{-1} at 150 mM NaCl and 4:1 PC/PS; $K_1 = 3.8 \times 10$ M^{-1} at 230 mM NaCl and 2:1 PC/PS; $K_1 = 1.3 \times 10$ M^{-1} at 230 mM NaCl and 4:1 PC/PS). The apparent dissociation constant ($1/K_1$) shifts to higher lipid concentrations if the percent of anionic lipid is decreased or the NaCl concentrations are increased (Figure 8B,C). Therefore, electrostatic forces likely define the association between MjK2cd and liposomes through ionic charge interactions and can be shielded by an increased ionic strength. Charge-dependent membrane−protein interactions are often a result of an electrostatic interaction between a basic region of a protein and a negatively charged membrane surface.

Lipid Specificity Screen. Does MjK2 binding to membranes display some specificity for a particular lipid? Lipids blotted onto nitrocellulose can be incubated with proteins to determine relative binding affinity. Proteins, which bind to the lipid spots, are detected using antibodies. A variety of lipids on home and commercial lipid blot screens were tested for their ability to bind MjK2cd (Figure 9). Blot results are not quantitative but do yield some information about the protein's relative affinity for various lipids. Little or no lipid binding was observed for the neutral polar lipids (PC, PE, and SIP) and for the mainly neutral lipid mixes (asolectin and polar lecithin). The major differences were observed for

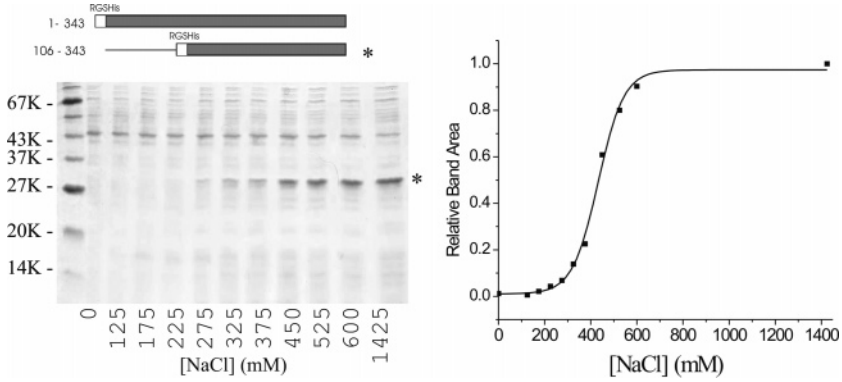

FIGURE 6: MjK2cd solubilization with NaCl. The cytoplasmic domain construct, MjK2cd (one asterisk) (30 kDa), was extracted from the pelleted cell lysate by increasing the NaCl concentration of the solubilization buffer and visualized on a Coomassie-stained gel. An analysis of MjK2cd gel bands is plotted.

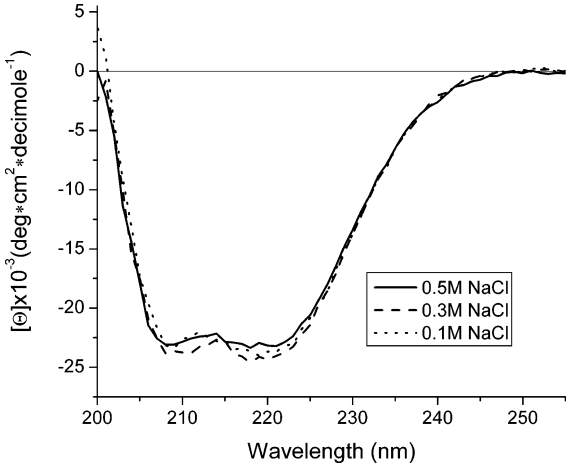

FIGURE 7: Circular dichroism spectra of MjK2cd. Spectra of MjK2cd were obtained in 10 mM phosphate (pH 7) and 0.5 M NaCl (—), 0.3 M NaCl (- - -), or 0.1 M NaCl (···). Spectra are averages of three individual scans obtained at room temperature.

lipids with single negative charges as the binding strength was in the order PA > PS > PG and PI, where PA had moderate binding and PI did not bind. Binding affinity was found to be strongest for PIPs and cardiolipin, which all contain more than one net negative charge. Although the interaction appears to be mainly electrostatic in nature, some difference in lipids with a single net negative charge should be noted. A specific activating lipid in the exotic membrane of *M. jannaschii*, composed of bipolar tetraether lipids, cannot yet be ruled out.

Modeling of MjK2cd and Positively Charged Regions. Alignments of MJK2 with MthK show that MJK2 is 29% identical and 55% similar to MthK over 91% of the MJK2 sequence. Similar membrane binding studies on the RCK domain of MthK suggest that it does not bind to anionic lipids (Figure 8B,C). In addition, there seems to be no requirement for high ionic strength in purification conditions for MthK (*9*). A sliding window plot of the residue charges for both MjK2 and MthK as well as for the average of 37 aligned K^+ channels with a single RCK domain found in the TIGR-CMR database (*30*) shows positive and negative charge differences along regions of the primary structure (Figure 10A). For MjK2, a higher positive charge density is found at the start of the RCK domain, at α-helices C and E in the RCK domain, from α-helix I to *β*-sheet H in the peripheral domain, and at the extreme C-terminus, and these are possible targets for electrostatic interactions with the membrane surface. A homology model of the MjK2 C-terminus dimer based on the MthK structure generated using Modeller (*31*) reveals the possible electrostatic surface potential for an octameric or tetrameric configuration (Figure 10C,D). A second tetrameric MjK2 model based on the conformational rearrangement of the RCK domains in the KTN model was also generated.

DISCUSSION

Cytoplasmic domains of membrane proteins are increasingly found to interact with lipids (*32*). Although membrane−protein interactions can be structural in nature, the proximity of a membrane-tethered cytoplasmic domain to the two-dimensional lipid bilayer makes membrane-delimited signaling highly efficient. Cytoplasmic domains from inward-

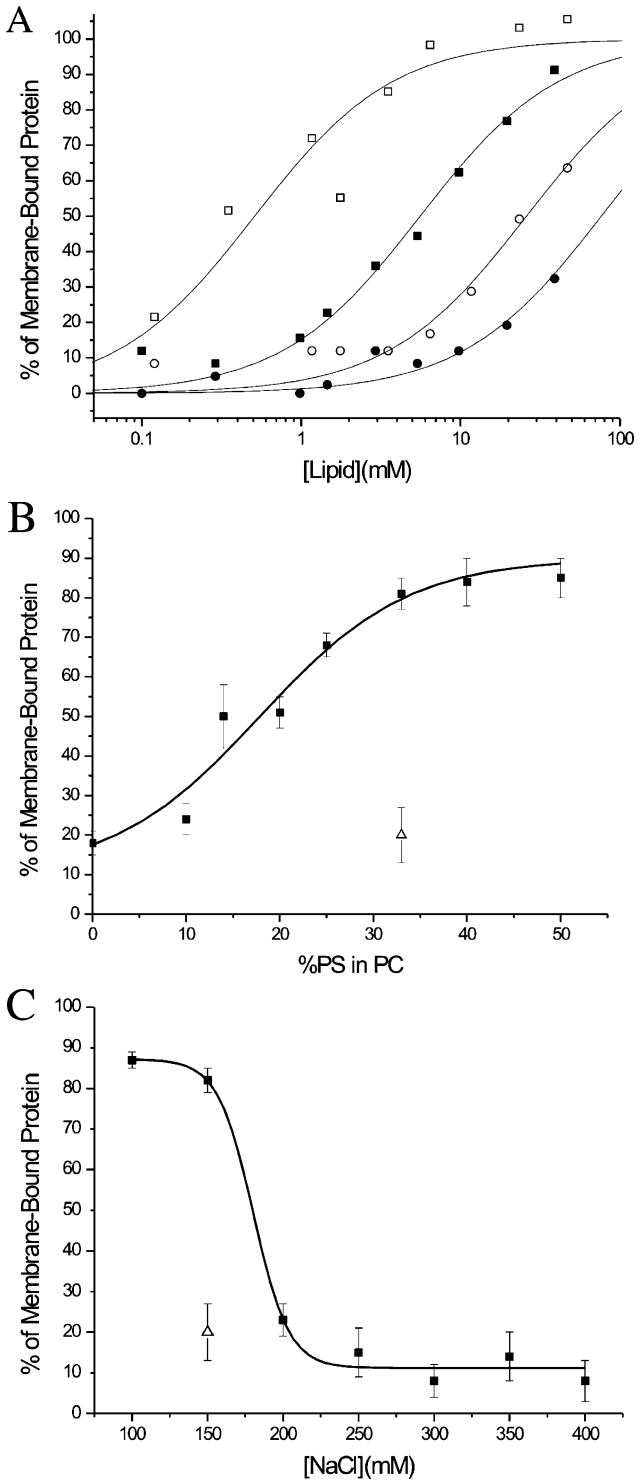

FIGURE 8: Binding of MjK2cd to liposomes. Purified MjK2cd was labeled with the fluorophore, CPM, and incubated with sucrose-loaded extruded PC/PS vesicles. The vesicles were centrifuged, and the supernatant of the unbound protein was measured for fluorescence. The amount of bound MjK2cd was determined by subtracting the unbound measurement from the fluorescent value of the supernatant in the absence of lipid. (A) The percentage of bound MjK2cd is plotted vs lipid concentration at 150 mM NaCl in 2:1 PC/PS vesicles (□), at 150 mM NaCl in 4:1 PC/PS vesicles (■), at 230 mM NaCl in 2:1 PC/PS vesicles (○), and at 230 mM NaCl in 4:1 PC/PS vesicles (●). (B) At 8 mM lipid and 150 mM NaCl, the binding of MjK2cd (■) to mixed liposomes at varying PC:PS ratios is plotted. (C) The fraction of MjK2cd (■) bound is plotted at increasing NaCl concentrations for 8 mM lipid and 2:1 PC/PS vesicles. In both panels B and C, data for MthKcd (△) binding at 8 mM lipid and 150 mM NaCl in 2:1 PC/PS vesicles are plotted.

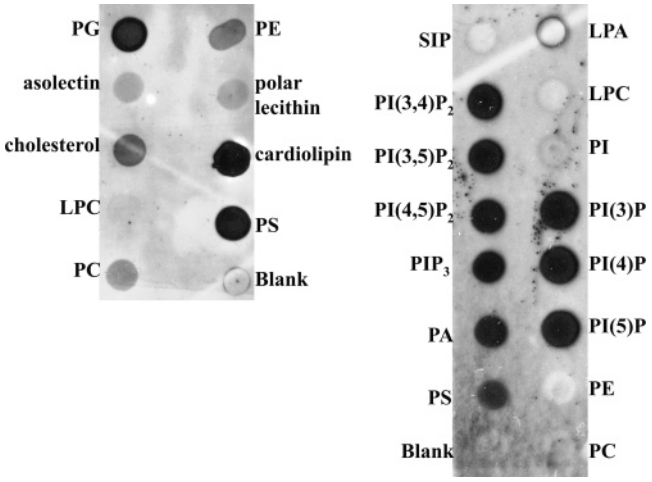

FIGURE 9: Lipid specificity blots for MjK2cd. A commercial ("PIP-StripsTM"; P-6001, Echelon Biosciences Inc., Salt Lake City, UT) PIP_2 lipid binding screen along with an in-house screen give increased intensities when MjK2cd binds to the lipid spots. MjK2cd binding was detected using anti-His antibodies.

rectifying K^+ channels and TRPV1 channels as well as the inactivating ball peptide from delayed rectifier Shaker-like channels are regulated by and interact with PIP_2 (*6*, *33*, *34*). In this paper, we show that solubilization of both MjK2 and MjK2cd is controlled by the concentration of salt in the extraction buffer. The cytoplasmic domain, properly folded as suggested by CD, is therefore responsible for the salt-dependent solubilization.

Basic proteins and peptides bind to phospholipid surfaces by interacting electrostatically with anionic lipids. The molar partition coefficient of MjK2cd ($K_1 \approx 10^3$ M^{-1}) for 2:1 PC/PS vesicles at 150 mM NaCl is on the same order of magnitude as those of basic peptides, pentalysine, and the nonmyristylated N-terminus of Src(2−16), which electrostatically associate with vesicles under similar conditions (100 mM KCl) (*35*, *36*). A decrease in the extent of vesicle association at a lower percentage of negative lipid or a higher salt concentration is typical of electrostatic binding. Myristylated Src(2−16) requires both myristylation ($K_1 \approx 10^4$ M^{-1}) and the N-terminal basic residues ($K_1 \approx 10^3$ M^{-1}) to be securely attached to membranes with a K_1 of $\approx 10^7$ M^{-1} (*35*, *37*). The addition of membrane targeting groups multiplies the association constant so both oligomerization and attachment by a transmembrane domain would greatly enhance the interaction of a single MjK2 cytoplasmic domain with negative lipids. The internal K^+ concentration of nonhalophilic archaea, like *M. jannaschii*, is higher than in most bacteria (>0.5 M) (*38*), and at the high salt level present under native conditions, the electrostatic contribution of a single MjK2 cytoplasmic domain would not be enough to stabilize its positioning at the membrane surface. The predicted MjK2 structure suggests that both a forced proximity to the membrane and a multimeric structure of the channel could more tightly fasten the domain to the nearby lipids. However, a transient interaction, only when internal salt levels decrease, could have a significant effect on the location of the cytoplasmic domain in relation to the membrane surface and channel. Any forces exerted on the channel's gate could influence function. By increasing the local concentration of the basic proteins within a few angstroms of the membrane, an electrostatic interaction could be a way for the second gene product to quickly associate with the channel and facilitate rapid channel assembly or could be an additional driving force for membrane insertion of an assembled channel (Figure 10B).

Although we have been unable to identify activators of MjK2, our data show that MjK2 mediates a low level of K^+ conductance, supporting a functionally closed channel. Previous findings for MjK2 are consistent with the low level of rescue that we observe using LB2003 cells (*16*, *21*). A similar level of rescue is also produced by KcsA expression, as specific requirements for low pH levels (*18*) keep KcsA in a closed confirmation under the conditions defined by the cytoplasm of *E. coli*, which suggests that a closed channel can leak enough potassium to rescue potassium uptake deficient cells at moderate KCl levels (*17*). MjK2 may also lack the proper conditions in *E. coli* to promote channel opening. When overexpressed, the native RCK-containing K^+ channel in *E. coli*, Kch, is also closed. Both Kch and MjK2 genes express a second orf just before the RCK domain, but the function of this gene product is still being debated. Our results with MjK2 M99L, as well as previous results with Kch mutants (*23*), show that there is no difference in the ability of the channel with or without the second gene product to weakly recover LB2003 cells, suggesting that MjK2 remains functional and closed. The structure of MthK, the only other K^+ channel shown to have the internal methionine start site, supports an integral role for the RCK domain in gating function (*9*). Thus, the inability of *in vivo* functional deletions of the second orf to affect the function of the channel does not rule out a physiological role for the second gene product. The preference for the location of the His tag suggests that an N-terminal His tag is either preventing the cytoplasmic domain from achieving the proper conformation for opening or directly occluding the ion conduction pathway.

While we are still investigating the regulation of MjK2, it may be possible that the lipid composition has an impact on function. Further studies must be carried out to determine if anionic lipids have an effect on MjK2 function. The specificity of lipid−protein interactions is often noted in the case of activating lipids. Although MjK2cd interacts more strongly with lipids with higher negative charges, there is little specificity beyond charge (Figure 9) (*39*). Because of the nature of life at extreme temperatures and pressures, the lipids of archaea differ from eukaryotic lipids. They are typically ether-linked isoprenoid acyl chains, often arranged as a single bipolar phospholipid (sometimes with different polar heads), forming a monolayer membrane. Therefore, specificity of an *M. jannaschii* protein for eukaryotic lipids should not be expected. Although some common eukaryotic headgroups, like phosphoethanolamine, are also found in *M. jannaschii*, headgroups contain a wide range of glycosylations (*40*). Identification of all *M. jannaschii* negatively charged lipids found at all growth conditions may be necessary to find whether specific lipids are involved in membrane signaling pathways.

Clues to the nature of the electrostatic membrane interaction were revealed by an analysis of the MjK2 primary sequence. The final seven residues are all lysines except for the final residue, a leucine. Polylysine stretches in proteins have been shown to bind to phospholipid membranes electrostatically and may play a role in orienting the

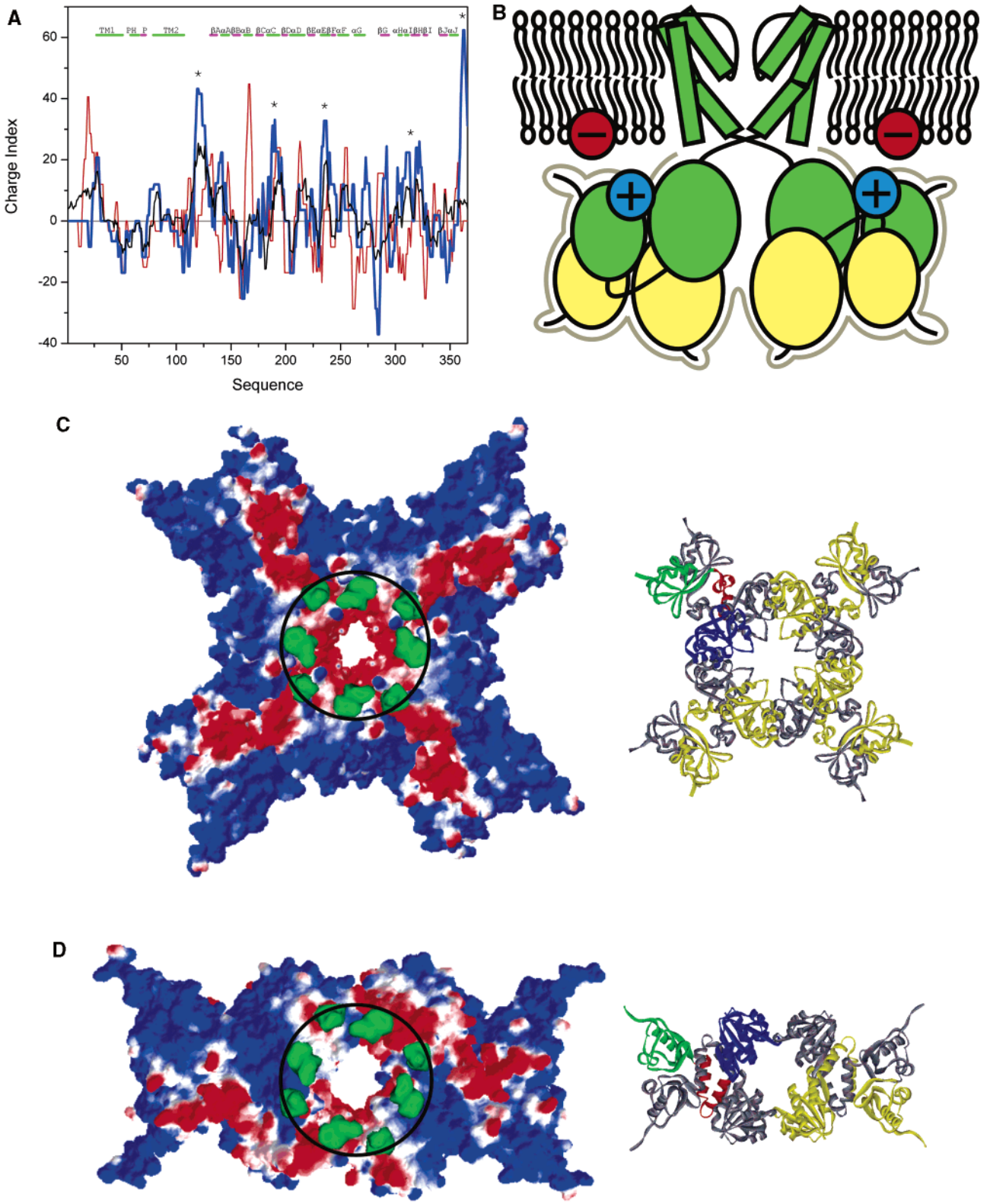

FIGURE 10: Electrostatic insights into the membrane interaction of MjK2. (A) A window of seven amino acids was used to calculate a charge index plot along the primary sequence of two-transmembrane segment RCK domain-containing channels. Regions of the MjK2 (blue) plot are indicated to highlight potentially important charge differences with MthK (red) and other two-transmembrane segment RCK domain-containing K^+ channels (average of 37, black). (B) The cartoon depicts the electrostatic interaction between the negatively charged membranes and a possible arrangement of MjK2. (C) An octamer of the RCK domain from MjK2 was modeled on the basis of the octamer of the RCK domains from the open MthK channel structure. The protein surface is viewed as the protein would face the lipid. The final three residues of the transmembrane segments from MthK are shown in green to signify the membrane region that cannot be accessed by the cytoplasmic domain. An electrostatic surface was generated mapping positive (blue) and negative (red) regions. (D) A tetrameric model of the RCK domain from MjK2 was modeled on the basis of the dimer-of-dimers model presented for the Ktn oligomeric structure. For both panels C and D, a small ribbon diagram is shown to illustrate the position of the dimers under the electrostatic surface map. Each dimer contains a yellow and a gray monomeric subunit except one yellow subunit in each multimer has been colored to indicate the RCK domain (blue), the peripheral domain (green), and the connecting helices (red).

cytoplasmic domain on the membrane (*41*, *42*). Although six residues are probably not sufficient to allow binding of MjK2cd to the membrane, the cytoplasmic domain has a high percentage of basic residues overall (43 Arg and Lys, 18%) which clearly should also contribute to membrane binding.

With the recently determined structure of MthK, a structural model for MjK2 can be generated. Upon first glance at the MthK structure, it is difficult to imagine how the large octameric RCK domain would interact with a membrane. A representation of an MjK2 octamer based on the MthK crystal structure displays the electrostatic potential of the surface facing the membrane (Figure 10C). In the structure, the octamer is rather close to the location of a membrane bilayer suggested by the final residues of the inner transmembrane helix. The transmembrane segments only cover a small area of the phospholipid headgroups accessible to a membrane-docked octameric RCK domain. The possibility also exists that the RCK domain of MjK2 adopts a slightly wider octameric conformation, allowing for greater interaction with the membrane.

Though similar to that of RCK domains, a different oligomeric structural arrangement has been proposed for the Ktn domains (*11*). The Ktn domain from the K^+ efflux system, KefC, is thought to be a tetramer, formed as a dimer of dimers. The tetrameric arrangement would exclude the second gene product and only be composed of channel-forming subunits. A surface map of the electrostatic potential of a putative tetrameric arrangement is shown in Figure 10D. Even though the tetramer is positioned closer to the base of the channel domain, a significant area of lipid would still be accessible to the cytoplasmic domains. However, a second tetrameric model, based on movements that would align hydrophobic pockets on the RCK domain (*11*), positions the tetramer more tightly under the channel and provides little access to the membrane. The tetrameric model may represent an alternate conformation of the cytoplasmic domain when the second gene product is not available. Regardless of the oligomeric state of the RCK domain in a functional channel, MjK2's RCK domain's electrostatic interaction with anionic lipids appears to be important in its biochemistry and could influence the cytoplasmic domain's central role in ligand-dependent gating.

ACKNOWLEDGMENT

We thank E. P. Bakker for the generous gift of the LB2003 *E. coli* strain, A. C. Dunsmoor-Ptak in D. Hunt's laboratory for mass spectrometry data, D. Wang for help using the CD spectrometer, T. Roosild for providing the coordinates for the KTN domain tetramer model, and the members of the Perozo laboratory for helpful discussions.

REFERENCES

1. Jan, L. Y., and Jan, Y. N. (1997) Cloned potassium channels from eukaryotes and prokaryotes, *Annu. Rev. Neurosci. 20*, 91−123.
2. Reuveny, E., Slesinger, P. A., Inglese, J., Morales, J. M., Iniguez-Lluhi, J. A., Lefkowitz, R. J., Bourne, H. R., Jan, Y. N., and Jan, L. Y. (1994) Activation of the cloned muscarinic potassium channel by G protein $\beta\gamma$ subunits, *Nature 370*, 143−146.
3. Wickman, K. D., Iniguez-Lluhl, J. A., Davenport, P. A., Taussig, R., Krapivinsky, G. B., Linder, M. E., Gilman, A. G., and Clapham, D. E. (1994) Recombinant G-protein $\beta\gamma$ subunits activate the muscarinic-gated atrial potassium channel, *Nature 368*, 255−257.
4. Hilgemann, D. W., and Ball, R. (1996) Regulation of cardiac Na^+, Ca^{2+} exchange and KATP potassium channels by PIP_2, *Science 273*, 956−959.
5. Fan, Z., and Makielski, J. C. (1997) Anionic phospholipids activate ATP-sensitive potassium channels, *J. Biol. Chem. 272*, 5388−5395.
6. Huang, C. L., Feng, S., and Hilgemann, D. W. (1998) Direct activation of inward rectifier potassium channels by PIP_2 and its stabilization by $G\beta\gamma$, *Nature 391*, 803−806.
7. Lopes, C. M., Zhang, H., Rohacs, T., Jin, T., Yang, J., and Logothetis, D. E. (2002) Alterations in conserved Kir channel-PIP_2 interactions underlie channelopathies, *Neuron 34*, 933−944.
8. Derst, C., and Karschin, A. (1998) Evolutionary link between prokaryotic and eukaryotic K^+ channels, *J. Exp. Biol. 201*, 2791−2799.
9. Jiang, Y., Lee, A., Chen, J., Cadene, M., Chait, B. T., and MacKinnon, R. (2002) Crystal structure and mechanism of a calcium-gated potassium channel, *Nature 417*, 515−522.
10. Jiang, Y., Pico, A., Cadene, M., Chait, B. T., and MacKinnon, R. (2001) Structure of the RCK domain from the *E. coli* K^+ channel and demonstration of its presence in the human BK channel, *Neuron 29*, 593−601.
11. Roosild, T. P., Miller, S., Booth, I. R., and Choe, S. (2002) A mechanism of regulating transmembrane potassium flux through a ligand-mediated conformational switch, *Cell 109*, 781−791.
12. Quirk, J. C., and Reinhart, P. H. (2001) Identification of a novel tetramerization domain in large conductance K_{Ca} channels, *Neuron 32*, 13−23.
13. Xia, X. M., Zeng, X., and Lingle, C. J. (2002) Multiple regulatory sites in large-conductance calcium-activated potassium channels, *Nature 418*, 880−884.
14. Shi, J., Krishnamoorthy, G., Yang, Y., Hu, L., Chaturvedi, N., Harilal, D., Qin, J., and Cui, J. (2002) Mechanism of magnesium activation of calcium-activated potassium channels, *Nature 418*, 876−880.
15. Bult, C. J., White, O., Olsen, G. J., Zhou, L., Fleischmann, R. D., Sutton, G. G., Blake, J. A., FitzGerald, L. M., Clayton, R. A., Gocayne, J. D., Kerlavage, A. R., Dougherty, B. A., Tomb, J. F., Adams, M. D., Reich, C. I., Overbeek, R., Kirkness, E. F., Weinstock, K. G., Merrick, J. M., Glodek, A., Scott, J. L., Geoghagen, N. S., and Venter, J. C. (1996) Complete genome sequence of the methanogenic archaeon, *Methanococcus jannaschii*, *Science 273*, 1058−1073.
16. Hellmer, J., and Zeilinger, C. (2003) MjK1, a K^+ channel from *M. jannaschii*, mediates K^+ uptake and K^+ sensitivity in *E. coli*, *FEBS Lett. 547*, 165−169.
17. Irizarry, S. N., Kutluay, E., Drews, G., Hart, S. J., and Heginbotham, L. (2002) Opening the KcsA K^+ channel: Tryptophan scanning and complementation analysis lead to mutants with altered gating, *Biochemistry 41*, 13653−13662.
18. Cuello, L. G., Romero, J. G., Cortes, D. M., and Perozo, E. (1998) pH-dependent gating in the *Streptomyces lividans* K^+ channel, *Biochemistry 37*, 3229−3236.
19. Buser, C. A., and McLaughlin, S. (1998) Ultracentrifugation technique for measuring the binding of peptides and proteins to sucrose-loaded phospholipid vesicles, *Methods Mol. Biol. 84*, 267−281.
20. Kavran, J. M., Klein, D. E., Lee, A., Falasca, M., Isakoff, S. J., Skolnik, E. Y., and Lemmon, M. A. (1998) Specificity and promiscuity in phosphoinositide binding by pleckstrin homology domains, *J. Biol. Chem. 273*, 30497−30508.
21. Sesti, F., Rajan, S., Gonzalez-Colaso, R., Nikolaeva, N., and Goldstein, S. A. (2003) Hyperpolarization moves S4 sensors inward to open MVP, a methanococcal voltage-gated potassium channel, *Nat. Neurosci. 6*, 353−361.
22. Farabaugh, P. J. (1978) Sequence of the lacI gene, *Nature 274*, 765−769.
23. Kuo, M. M., Saimi, Y., and Kung, C. (2003) Gain-of-function mutations indicate that *Escherichia coli* Kch forms a functional K^+ conduit in vivo, *EMBO J. 22*, 4049−4058.
24. Martin, S. E., Shabanowitz, J., Hunt, D. F., and Marto, J. A. (2000) Subfemtomole MS and MS/MS peptide sequence analysis using nano-HPLC micro-ESI Fourier transform ion cyclotron resonance mass spectrometry, *Anal. Chem. 72*, 4266−4274.
25. Garty, H., Rudy, B., and Karlish, S. J. (1983) A simple and sensitive procedure for measuring isotope fluxes through ion-specific channels in heterogenous populations of membrane vesicles, *J. Biol. Chem. 258*, 13094−13099.

26. Cserzo, M., Wallin, E., Simon, I., von Heijne, G., and Elofsson, A. (1997) Prediction of transmembrane α-helices in prokaryotic membrane proteins: The dense alignment surface method, *Protein Eng. 10*, 673−676.
27. Combet, C., Blanchet, C., Geourjon, C., and Deleage, G. (2000) NPS@: Network protein sequence analysis, *Trends Biochem. Sci. 25*, 147−150.
28. Johnson, W. C. (1999) Analyzing protein circular dichroism spectra for accurate secondary structures, *Proteins 35*, 307−312.
29. Sreerama, N., and Woody, R. W. (1993) A self-consistent method for the analysis of protein secondary structure from circular dichroism, *Anal. Biochem. 209*, 32−44.
30. Peterson, J. D., Umayam, L. A., Dickinson, T., Hickey, E. K., and White, O. (2001) The Comprehensive Microbial Resource, *Nucleic Acids Res. 29*, 123−125.
31. Fiser, A., and Sali, A. (2003) Modeller: Generation and refinement of homology-based protein structure models, *Methods Enzymol. 374*, 461−491.
32. Hilgemann, D. W., Feng, S., and Nasuhoglu, C. (2001) The complex and intriguing lives of PIP_2 with ion channels and transporters, *Sci. STKE 2001*, RE19.
33. Prescott, E. D., and Julius, D. (2003) A modular PIP_2 binding site as a determinant of capsaicin receptor sensitivity, *Science 300*, 1284−1288.
34. Oliver, D., Lien, C. C., Soom, M., Baukrowitz, T., Jonas, P., and Fakler, B. (2004) Functional conversion between A-type and delayed rectifier K^+ channels by membrane lipids, *Science 304*, 265−270.
35. Buser, C. A., Sigal, C. T., Resh, M. D., and McLaughlin, S. (1994) Membrane binding of myristylated peptides corresponding to the NH_2 terminus of Src, *Biochemistry 33*, 13093−13101.
36. Kim, J., Mosior, M., Chung, L. A., Wu, H., and McLaughlin, S. (1991) Binding of peptides with basic residues to membranes containing acidic phospholipids, *Biophys. J. 60*, 135−148.
37. Sigal, C. T., Zhou, W., Buser, C. A., McLaughlin, S., and Resh, M. D. (1994) Amino-terminal basic residues of Src mediate membrane binding through electrostatic interaction with acidic phospholipids, *Proc. Natl. Acad. Sci. U.S.A. 91*, 12253−12257.
38. Martin, D. D., Ciulla, R. A., and Roberts, M. F. (1999) Osmoadaptation in archaea, *Appl. Environ. Microbiol. 65*, 1815−1825.
39. Rohacs, T., Lopes, C. M., Jin, T., Ramdya, P. P., Molnar, Z., and Logothetis, D. E. (2003) Specificity of activation by phosphoinositides determines lipid regulation of Kir channels, *Proc. Natl. Acad. Sci. U.S.A. 100*, 745−750.
40. Sprott, G. D. (1992) Structures of archaebacterial membrane lipids, *J. Bioenerg. Biomembr. 24*, 555−566.
41. Victor, K. G., and Cafiso, D. S. (2001) Location and dynamics of basic peptides at the membrane interface: Electron paramagnetic resonance spectroscopy of tetramethyl-piperidine-N-oxyl-4-amino-4-carboxylic acid-labeled peptides, *Biophys. J. 81*, 2241−2250.
42. Murray, D., Arbuzova, A., Hangyas-Mihalyne, G., Gambhir, A., Ben-Tal, N., Honig, B., and McLaughlin, S. (1999) Electrostatic properties of membranes containing acidic lipids and adsorbed basic peptides: Theory and experiment, *Biophys. J. 77*, 3176−3188.

BI048390F